Journal of Thermal Analysis, Vol. 36 (1990) 1867-1888

DESCRIPTION OF THE SHAPE OF THERMOANALYTICAL CURVES

[1]G. Pokol, [2]F. Hevesi Tóth, [3]I. Péter, [1]J. Madarász, [1]T. Kocsis and *[1]S. Gál*

[1]INSTITUTE FOR GENERAL AND ANALYTICAL CHEMISTRY, TECHNICAL UNIVERSITY OF BUDAPEST, 1521 BUDAPEST, HUNGARY
[2]MINISTRY OF THE INTERIOR, P.O.B. 314/32, 1903 BUDAPEST, HUNGARY
[3]G. RICHTER CHEMICAL WORKS, P.O.B. 27, 1475 BUDAPEST, HUNGARY

Empirical parameters were chosen for the characterization of peaks (or steps) of thermoanalytical curves. The parameters were applied in studies on the repeatability, the relationship between kinetic constants and peak shape, the effect of sample thermal resistance. Kinetic constants can be estimated on the basis of peak shape parameters. Besides, approximate criteria were formulated for experiments allowing kinetic evaluation with the neglect of the heat transport within the sample. The empirical parameters were also used in checking the suitability of DSC data for purity analysis and in detecting changes of the thermal decomposition of papers caused by ageing.

The possible goals of thermoanalytical investigations may be classified into three basic directions:

a. analysis of composition (including identification of components and quantitative determinations),

b. estimation of physical or chemical parameters (temperatures and heats of transformations, specific heat, thermal expansion coefficient, etc.), and

c. characterization of physical and chemical transformations (kinetics and mechanism of reactions).

Whichever the goal is, the evaluation of the measured thermoanalytical curves involves some description of curve shape. The description is often qualitative, in order to answer whether a reaction is simple or consists of several steps, whether it is reversible or not, etc. However, the demand for a quantitative characterization is increasing, and there are important cases (as kinetics) when it is essential.

The analysis of the shape of thermoanalytical curves may be carried out either by model/curve fitting or calculating characteristic quantities. The present work is concerned with the latter way.

John Wiley & Sons, Limited, Chichester
Akadémiai Kiadó, Budapest

A number of authors applied numerical quantities to characterize the shape of peaks (or steps) belonging to chemical reactions and to determine kinetic parameters. As classical examples, let us mention Kissinger's work [1] using a shape index to estimate formal order of reaction, and the shape and reaction type indices of Koch [2, 3] applied also in non-isothermal kinetics.

Várhelyi and Székely found that the three parameters of the usual kinetic equation (apparent activation energy, pre-exponential factor and apparent order) can be estimated on the basis of the position, width and the degree of asymmetry of a peak [4].

For several years, a project has been conducted to find different empirical parameters to describe the shape of non-isothermal thermoanalytical curves and to assess their applicability.

This paper gives an outline of the work done so far. On the one hand, it briefly summarizes those results which have been published before [5-8], and, on the other hand, it gives an account on some new applications.

Empirical parameters of peak shape

Table 1 lists the empirical parameters applied in the characterization of peaks of differential and derivative type thermoanalytical curves (DSC, DTA, DTG etc.). The same quantities can be used to evaluate steps of integral curves (TG), after numerical derivation. Throughout the discussion to follow, constant heating rate is assumed.

The calculation of the parameters must be preceded by baseline subtraction; smoothing of data may also be necessary. These operations may considerably influence the shape of the peak.

Some of the parameters are temperatures, transformation rates or reacted fractions (conversions) belonging to characteristic points of the peak as $T(\mathrm{Max})$, $T(\alpha)$, $\alpha(\mathrm{Max})$, etc. Others, like e.g. W_T, U or $R(\alpha)$ are derived from the quantities mentioned before. The third group of parameters consist of mathematical moments of the peak and quantities derived from them. The equations of the moments given in Table 1 are valid if the curve is given by a series of points evenly spread over the temperature axis.

Each parameter listed in Table 1 relates to one of four properties of the peak:

a. position of the peak along the temperature axis: $T(\mathrm{Max})$, $T(\alpha)$, M_{1R}

b. width: $\Delta T(\alpha 2, \alpha 1)$ W_T, C_2

c. asymmetry: $\alpha(\mathrm{Max})$, $R(\alpha)$, $R(\mathrm{Max})$, s
d. sharpness/flatness of the peak: U, e

Table 1 Empirical parameters for the description of peak shape

$T(\mathrm{Max})$	temperature of the peak maximum
$T(\alpha)$	temperature relevant to a particular reacted fraction (α)
$T(i_1)$, $T(i_2)$	temperature of inflexion points
$W_T = (\mathrm{d}\alpha/\mathrm{d}T)^{-1}_{\mathrm{Max}}$	the reciprocal of the maximum rate of transformation
$\Delta T(\alpha_2, \alpha_1) = T(\alpha_2) - T(\alpha_1)$	
$U = \frac{\Delta T(0.8, 0.2)}{W_T}$	
$R(\alpha) = \frac{\Delta T(\alpha, 0.2)}{\Delta T(0.8, 0.2)}$	
$M_{1R} = \frac{\sum_j T_j y_j}{\sum_j y_j}$	the first relative moment of the peak; y–a signal proportional to the rate of transformation
$C_k = \frac{\sum_j (T_j - M_{1R})^k \cdot}{\sum_j y_j}$	the k-th relative central moment of the peak
$s = C_3/C_2^{3/2}$	the skewness of the peak
$e = C_4/C_2^2 - 3$	the "excess" (flatness) of the peak

Beyond parameters, e.g., $T(\mathrm{Max})$, generally used in the evaluation of thermoanalytical curves, there are some which had been applied in kinetic calculations, as $\alpha(\mathrm{Max})$ [4, 9, 10] or $\Delta T(\alpha_2, \alpha_1)$ [4]. Mathematical moments were also proposed for the characterization of DTA curves [11].

Repeatability of thermoanalytical curves. The effect of noises and baseline on peak shape.

Repeatability and reproducibility of characteristic temperature of transformations, heats of melting and solid-solid phase transitions have been thoroughly studied, especially in projects to select suitable substances for instrument calibration [12-19].

When conclusions are to be drawn from the progress of transformation as a function of time and temperature, the repeatability and reproducibility of curve shape is also of interest.

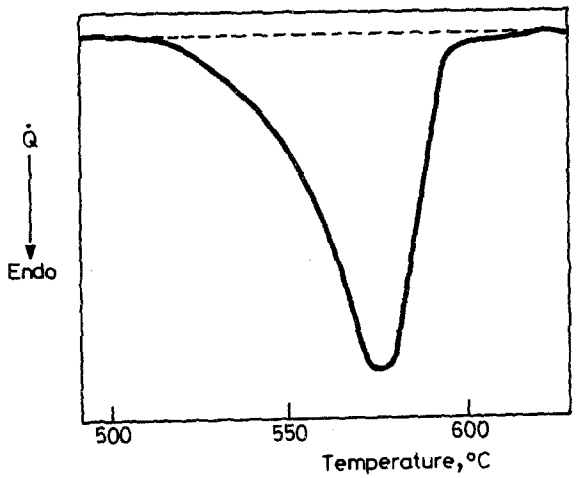

Fig. 1 DSC curve of a mineral gibbsite in flowing air with a heating rate of 10 deg/min

The empirical parameters mentioned before are suitable to compare experimental curves. As an example, the results of replicate DSC curves of mineral gibbsite decomposition are shown in Table 2. The evaluated peak reflects two reactions: a part of the gibbsite decomposes to boehmite (see the shoulder of the low-temperature side of the peak in Fig. 1), the majority transforms to an intermediate alumina [20].

$$Al(OH)_3 \text{ (gibbsite)} = Al\,O(OH) \text{ (boehmite)} + H_2O$$

$$2Al(OH)_3 \text{ (gibbsite)} = \chi - Al_2O_3 + 3H_2O$$

The standard deviations in Table 2 show a good repeatability for several parameters.

Standard deviations and trends of peak shape parameters were also applied in studies on the effect of noise level and baseline choice on the shape of smoothed and baseline corrected peaks [6]. The results were taken into account when selecting parameters which are repeatable and, at the same time, sensitive to meaningful differences.

Table 2 Averages, standard and relative standard deviations of some empirical parameters calculated from seven replicate DSC curves of mineral gibbsite

Parameter	average	s.d.	r.s.d, %
T(max), K	576	1	
T(0.2), K	554.6	0.5	
T(0.8), K	580.7	0.4	
ΔT (0.8,0.2), K	26.2	0.4	2
W_T, K	34.9	0.6	2
U	0.75	0.01	1
R(0.6)	0.729	0.003	0.4
R(Max)	0.80	0.02	3
M_{1R}, K	563.3	0.4	
$C_2 \cdot 10^{-2}$, K^2	2.56	0.08	0.8
$C_3 \cdot 10^{-3}$, K^3	-2.76	0.30	11
$C_4 \cdot 10^{-5}$, K^4	2.28	0.20	9
s	-0.67	0.05	7
e	0.47	0.11	23

Dependence of peak shape on kinetic constants

The relationship between the empirical quantities discussed above and the constants of the simple formal rate equation

$$d\alpha/dt = A \cdot \exp\left(-\frac{E}{RT}\right) \cdot (1-\alpha)^n \qquad (1)$$

was studied by means of mathematical modelling [7]. The influence of the preexponential coefficient (A), the apparent order of reaction (n) and the apparent activation energy (E) on the location, width and asymmetry of a peak is well known. The use of peak shape parameters offered a new possibility for the quantitative description of this influence.

The effect of the apparent energy of activation on parameters of peak location is demonstrated in Fig. 2 (with fixed heating rate and A); the relationship between the width and the preexponential factor is shown in Fig. 3. Generally speaking, the position of the peak is sensitive to the activation energy and the preexponential factor but only slightly sensitive to the formal order. The width depends on all the three kinetic constants. The parameters related to asymmetry and sharpness were found to be independent (or nearly independent) of E and A; their values are shown in Fig. 4 as functions of the apparent order.

If the formal order is fixed (or determined from the relationships demonstrated in Fig. 4) the two remaining kinetic constants can be estimated using a $\log A$ *vs.* E diagram. For this purpose, lines of levels of two empirical parameters, one related to peak position, the other to peak width, should be drawn in the diagram, as shown in Fig. 5. The diagram in the fig-

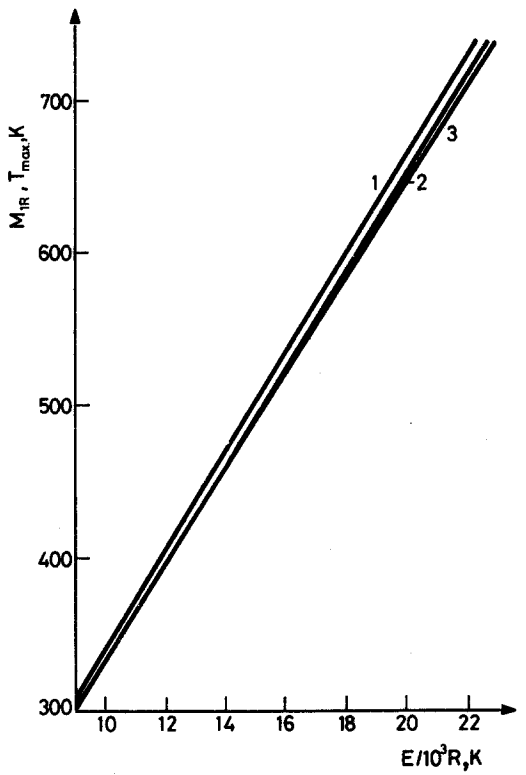

Fig. 2 The effect of the activation energy on parameters characterizing peak location. $A = 10^{11}$ s^{-1}, $dT/dt = 10$ deg/min. 1 - T(max) for $n = 2/3$ and $n = 1$; 2 - M_{1R} for $n = 1$; 3 - M_{1R} for $n = 2/3$

ure belongs to $n = 2/3$. If a peak with $M_{1R} = 551$ K and $W_T = 40$ K is evaluated, the solution, i.e. the values of E and A are given by the intersection of the two lines (point R). The procedure is suitable to determine a confidence internal for the solution, as well.

The borders of the confidence region are drawn in thick lines in the diagram assuming a ± 2 K uncertainty of W_T and ±5 K uncertainty of M_{1R}.

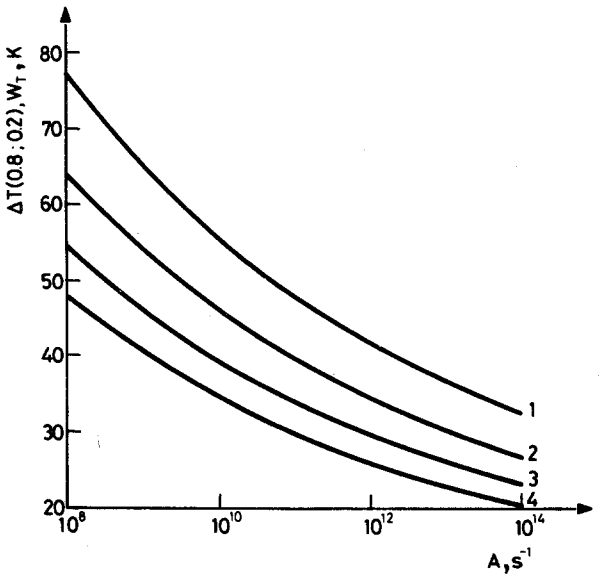

Fig. 3 The effect of the pre-exponential factor on parameters characterizing peak width. $E/R = 1.7 \cdot 10^4$ K, $dT/dt = 10$ deg/min. 1 - W_T for $n = 1$; 2 - W_T for $n = 2/3$; 3 - $\Delta T(0.8, 0.2)$ for $n = 1$; 4 - $\Delta T(0.8, 0.2)$ for $n = 2/3$

Visibly, the region containing the acceptable solutions is fairly extended and not coaxial, which points to the fact that the estimated values of the apparent activation energy and preexponential factor are not independent. This is a consequence of the mathematical nature of the Arrhenius equation, which has been found to be a source of the kinetic compensation effect [21-25].

If the formal order is not fixed, the confidence region will be three-dimensional in the $\log A$ - E - n space. Figure 6 shows the domain defined by the same values and uncertainties of M_{1R} and W_T (peak location and width) as in Fig. 5. The confidence region will be a part of this domain, its position and depth will be determined by the estimated value and uncertainty of the formal order.

The longitudinal axis of domains similar to the one in Fig. 6 is nearly linear and not parallel with the n axis, which reflects that the estimated formal order is also correlated to the other two constants (A and E) [26-28].

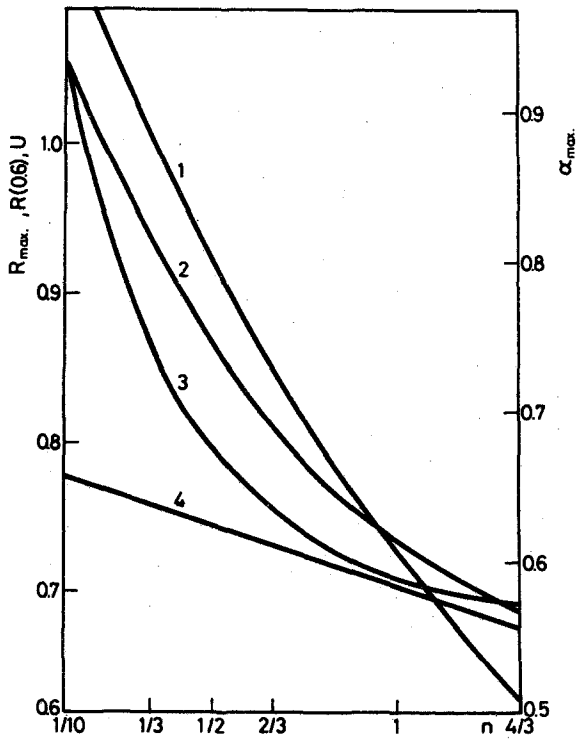

Fig. 4 The effect of the formal order of reaction on parameters related to sharpness and asymmetry of the peak. 1 - R(max); 2 - α(max); 3 - U; 4 - R(0.6)

The method for the estimation of kinetic constants based on the empirical parameters of peak shape was compared to least-squares model fitting. Depending on the nature of experimental errors, the latter may be of inferior efficiency. The discussion of the whole topic was published in Ref. 7.

The effect of sample thermal resistance on peak shape

Both diffusion and heat transport play an important role in the reactions of solids. In thermoanalytical experiments, thermal resistances occur between the heating element and the sample holder, in the wall of the latter, between the crucible and the sample and within the sample. One or more of these resistances often determine the overall rate of transformation.

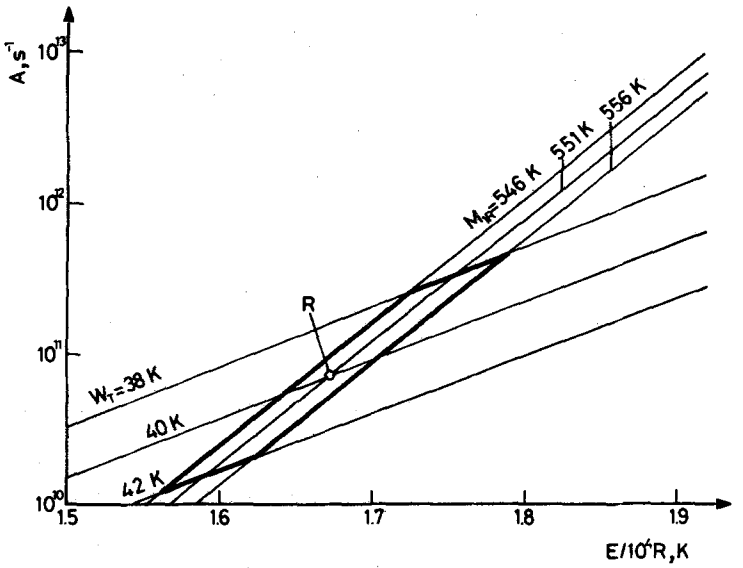

Fig. 5 Estimation of the pre-experimental factor and the activation energy by means of intersecting zones; $n = 2/3$

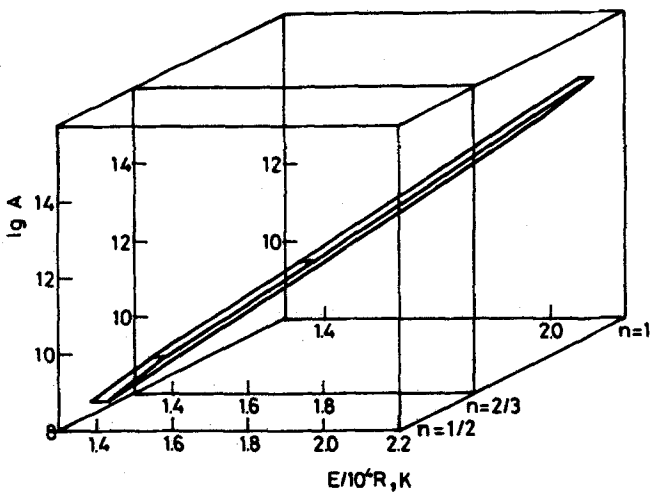

Fig. 6 The three-dimensional region defined by 546 K $\leq M_{1R} \leq$ 556 K and 38 K $\leq W_T \leq$ 42 K

For a detailed study, the thermal resistance within the sample was chosen, because it can hardly be intensified (though its influence can be diminished by a smaller sample size). The effect was investigated by means of a simple mathematical model of a solid$_1$ = solid$_2$ + gas phase boundary

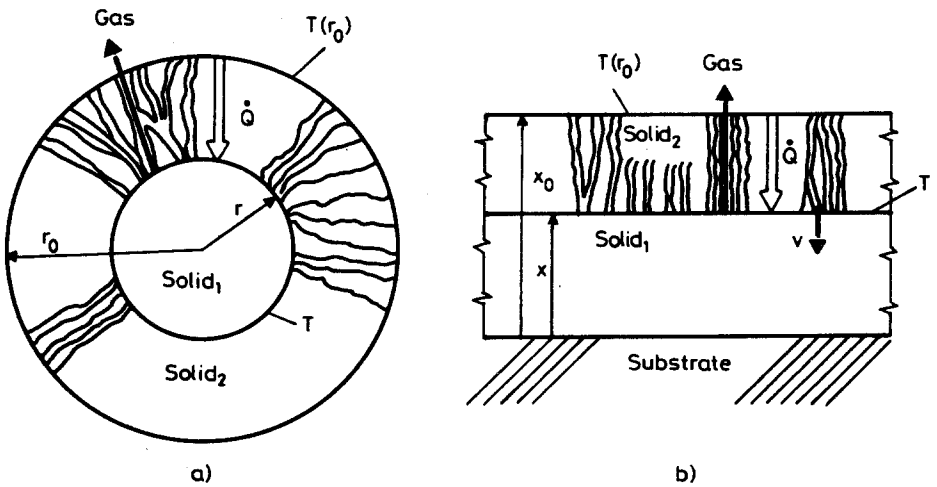

Fig. 7 The scheme of the system controlled by the chemical reaction and heat conduction through the product layer. Sample geometry: a - spherical or cylindrical; b - layer

reaction [8]. The rate of the transformation was assumed to be controlled by the chemical reaction at the reagent/product interface and the heat conduction from the external surface of the sample through the porous product layer to the reacting interface. The heat capacity of the sample was neglected, the heat required for the reaction was only taken into account. A scheme of the model system is shown in Fig. 7.

For a sphere, the rate of the reaction (in mole/s units) at time t can be expressed using the radius of the reacting phase boundary

$$\frac{dN}{dt} = 4r^2\pi A' \exp\left(-\frac{E}{RT}\right) \tag{2}$$

If the sample is a long, cylindrical rod, the expersion includes the length L:

$$\frac{dN}{dt} = 2\pi rL \cdot A' \exp\left(-\frac{E}{RT}\right) \tag{3}$$

where r denotes the radius of the reacting interface (a cylinder) at time t. In the case of a planar layer adhering to an inert substrate the rate is

$$\frac{dN}{dt} = S \cdot A' \exp\left(-\frac{E}{RT}\right) \tag{4}$$

where S is the surface area. The linear velocity of the reacting phase boundary can be obtained from the preceding equations using the actual area of the interface, the density ρ and the molar mass M of the starting material:

$$v = \frac{A' \cdot M}{\rho} \exp\left(-\frac{E}{RT}\right) \tag{5}$$

The heat flux to or from the reacting interface is the product of the rate and the heat of the reaction:

$$Q_r = \frac{dN}{dt} \cdot \Delta H \tag{6}$$

Being the same for all the three cases, Eqs 2-6 express the chemical control of the process. In order to describe the effect of the heat conduction from the external surface of the sample to the reacting interface, the difference between the temperature of the external surface ($T(r_o)$ or $T(x_o)$) and that of the reacting phase boundary (T) should be considered. The heat flux may then be formulated for the three-, two- and one-dimensional case

$$\dot{Q}_\lambda = 4\pi\lambda r_o r \frac{T(r_o) - T}{r_o - r} \quad \text{(sphere)}, \tag{7}$$

$$\dot{Q}_\lambda = 2\pi\lambda L \frac{T(r_o) - T}{\ln \frac{r_o}{r}} \quad \text{(cylinder)}, \tag{8}$$

$$\dot{Q}_\lambda = \lambda S \frac{T(x_o) - T}{x_o - x} \quad \text{(layer)} \tag{9}$$

where λ denotes the effective thermal conductivity of the product layer.

Simulated curves can be constructed form the above equations, taking into account that the heat effect of the reaction should equal the heat trans-

ferred to the reacting phase boundary, i.e., $\dot{Q}_V$ of Eq. 6 is equal to $\dot{Q}_\lambda$ of Eqs 7, 8 or 9. $T(r_o)$ was regarded to be adequate to the linear temperature program.

The other assumptions and simplifications of the model, the procedure of calculation and the results for the spherical model were discussed in detail in [8].

A set of curves generated with different thermal conductivities (and fixed other parameters) is presented in Fig. 8. Beyond the transformation rate, the difference between the temperatures and the reacting interface, i.e. temperature lag is also shown. The distorting effect of sample thermal resistance is clearly visible. For compact non-metallic materials the real range of thermal conductivity is below 10 $Wm^{-1}K^{-1}$, and, in the case of the model, the heat conducting layer is porous. On the other hand, the curves of Fig. 8 correspond to rather large samples (over 200 mg).

From curves simulated with different thermal conductivities, sample sizes, E and A values and heating rates the empirical parameters of peak shape were calculated and the maximum temperature lag was also established for each set of input parameters. From these data, the different peak shape parameters could be plotted as functions of a chosen input parameter. The relationship of the maximum temperature lag and sample size is demonstrated in Fig. 9 for different λ values.

The effect of thermal conductivity on a parameter assigned to the asymmetry of the peak is shown in Fig. 10. $R(0.6)$ can be applied to determine the formal order of reaction (see the preceding chapter and Fig. 4) which, in the discussed case, equals 2/3. If the effect of sample thermal resistance is neglected in the evaluation of kinetics, the distortion of peak shape will result in an error of the estimated n. If a maximum acceptable error is specified (in Fig. 10, the maximum error is 0.1), the corresponding shift of $R(0.6)$ can be established. A minimum of acceptable effective thermal conductivities can be obtained as shown in the figure provided the other parameters are fixed. If λ is less than the minimum, the error of the estimated apparent order will exceed the specified limit.

The relationships between material or experimental parameters and peak shape cannot be used in the form of plots like Figs 9 and 10 since, in a real series of investigations, several parameters are different in the individual experiments. For this reason, the results of model calculations were generalized by means of dimension analysis [8]. For the maximum temperature lag within the sample

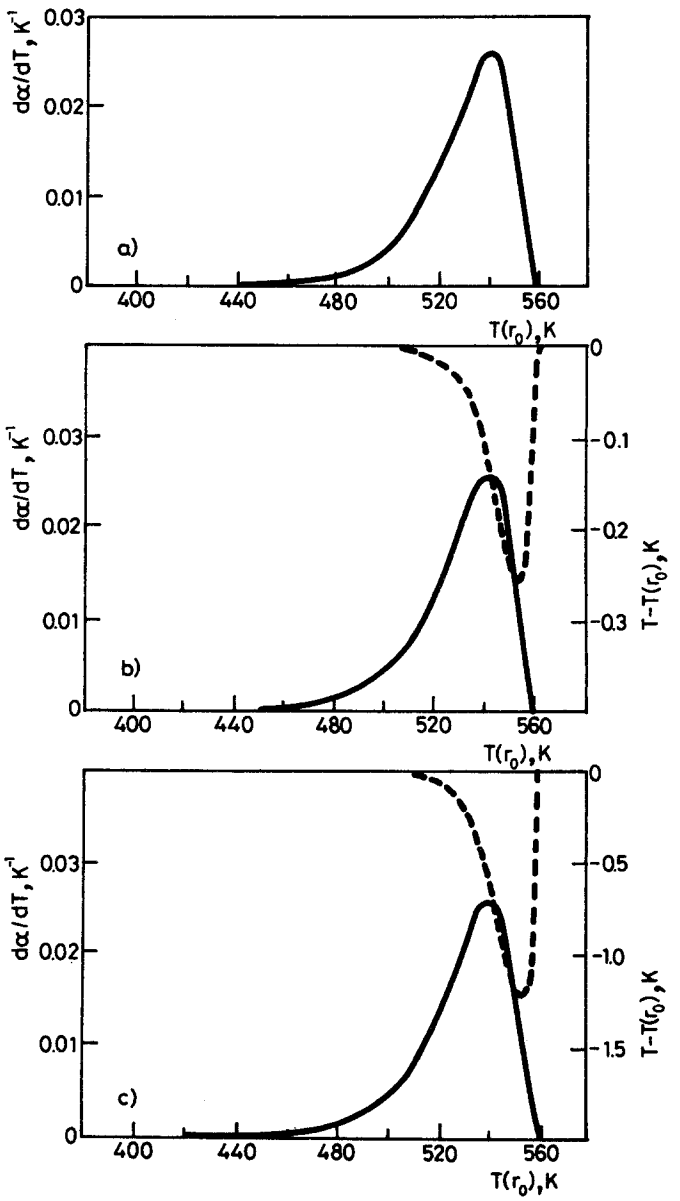

Fig. 8a-c Calculated curves of the transformation rate (—) and the difference between the temperature of the reacting interface and the program temperature (– – –) for a sample of 3 mm initial radius. $\lambda(WK^{-1}m^{-1})$ = a - ∞; b - 100; c - 20. The other input parameters: $A' = 4.72 \cdot 10^{12}$ mol $m^2 s^{-1}$; $E/R = 1.67 \cdot 10^4$ K; $\beta = 1/6$ deg/s; $M = 0.1$ kg/mol; $\rho = 2000$ kg/m^3; $\Delta H = 100$ kJ/mol

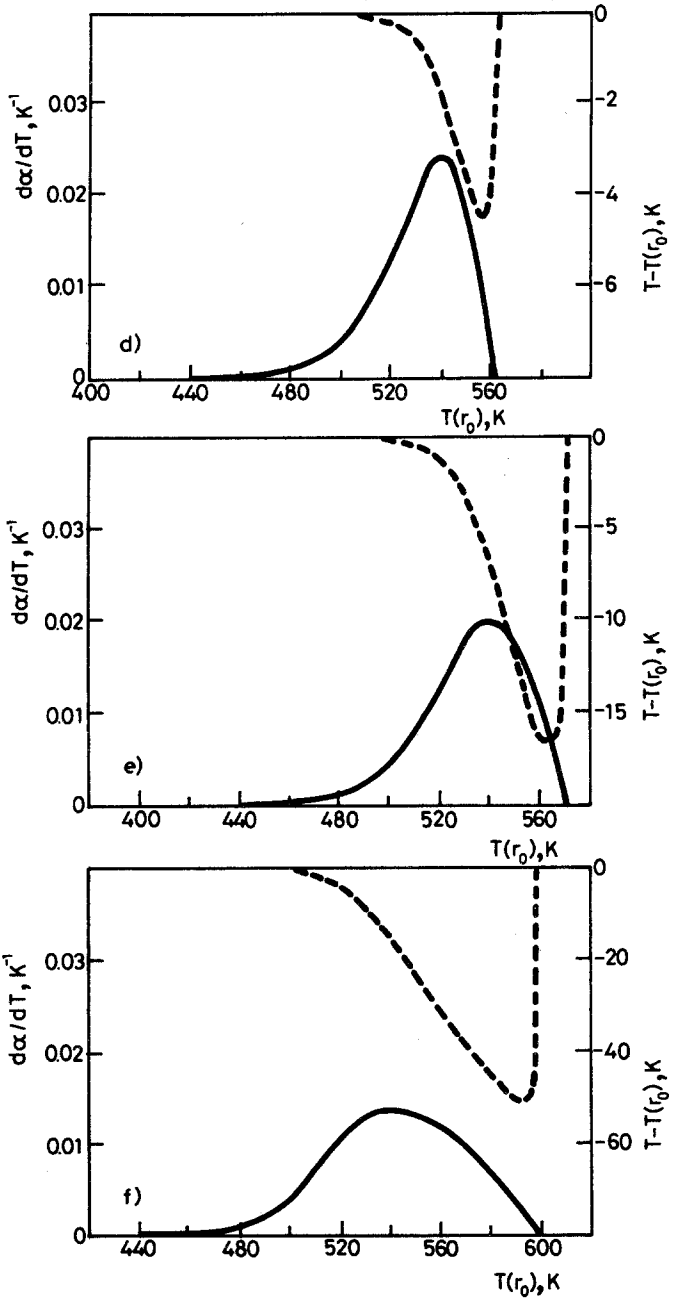

Fig. 8d-f Calculated curves of the transformation rate (—) and the difference between the temperature of the reacting interface and the program temperature (– – –) for a sample of 3 mm initial radius. $\lambda(WK^{-1}m^{-1})$ = d - 5; e - 1; f - 0.2. The other input parameters: $A' = 4.72 \cdot 10^{12}$ mol $m^2 s^{-1}$; $E/R = 1.67 \cdot 10^4$ K; $\beta = 1/6$ deg/s; $M = 0.1$ kg/mol; $\rho = 2000$ kg/m^3; $\Delta H = 100$ kJ/mol

$$l \cong \text{const.} \frac{r_0^2 H\beta}{W_T \lambda} \tag{10}$$

was obtained, where H denotes the heat of reaction in unit sample volume.

If kinetic calculations are carried out with the neglect of sample thermal resistance, the parameters should obey the

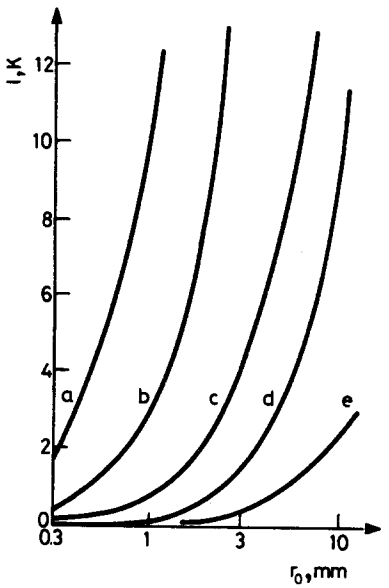

Fig. 9 The effect of sample radius on the maximum temperature lag. $\lambda(WK^{-1}m^{-1})$ = a - 0.2; b - 1; c - 5; d - 20-; e - 100. For the other parameters of simulation see the legend for Fig. 8

$$\frac{\lambda W_T^2}{r_0^2 H\beta} \geq \text{const.}' \tag{11}$$

criterion; the constant depends on the acceptable error limit. Relation (11) may be used in the design of experiments. An example for this was presented in Ref. 8.

Data checking prior to purity calculation

Since the empirical parameters of peak shape are easy to calculate they may be suitable for a preliminary checking of experimental data, prior to a more sophisticated quantitative evaluation. For this purpose, some simple criteria should be established whether the experimental curve is likely obeying the assumed physico-chemical model or not.

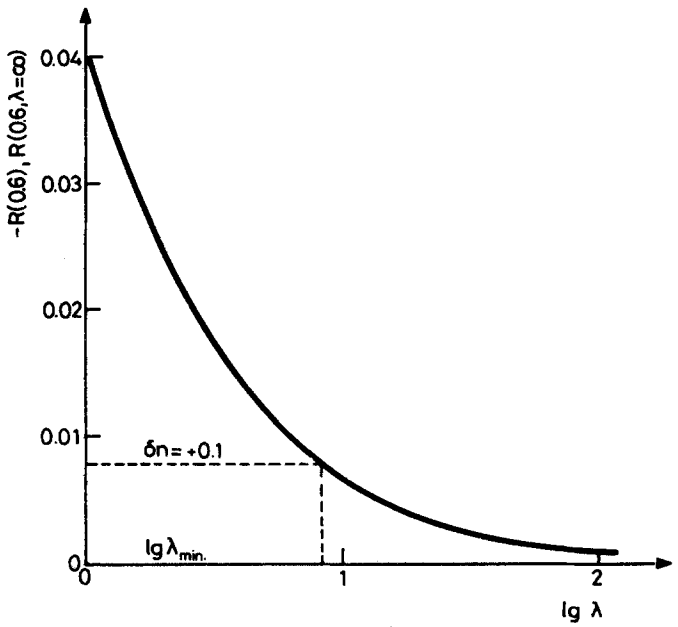

Fig. 10 The effect of thermal conductivity on the shift of $R(0.6)$ for a sample of 3 mm radius. For the other parameters see the legend for Fig. 8

Such an application may be checking DSC melting curves if they are suitable for purity analysis on the basis of the van't Hoff equation. Melting curves of a pharmaceutical substance with two different impurity levels are shown in Fig. 11. The shape of the peaks is typical for a eutectic system containing a small amount of one component: the ascending part of the curve lasts longer than the descending part and contains a nearly linear region. Curves of this type may be suitable for purity analysis.

The melting peak in Fig. 12 is quite symmetrical. Its shape is determined by a process different from melting point depression in a eutectic system (the main component and the impurity may, e.g., form a solid solution).

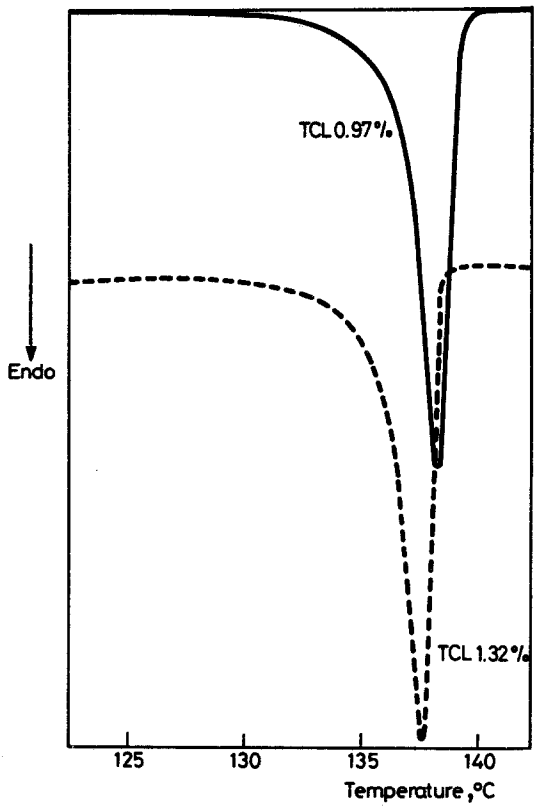

Fig. 11 Melting DSC curves of two cimetidin samples; heating rate: 1 deg/min. The impurity level determined with chromatography is also given

Such curves may be found using parameters related to peak asymmetry (see $T(\max)$-$T(0.5)$, $R(\max)$ and s in Table 3). Attempts to fit inadequate models to experimental data can be avoided in this way.

The effect of ageing on the thermal decomposition of paper

Thermal analysis is often applied to study complex systems or processes where a complete interpretation of the changes in thermal behaviour is impossible but it is important to detect trends of those changes.

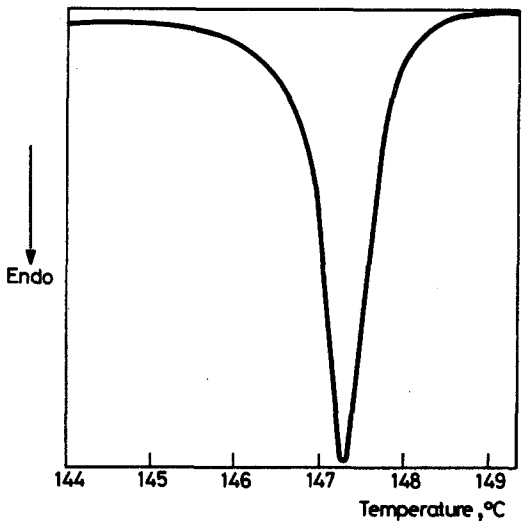

Fig. 12 Melting DSC curve of a ketoconazol sample. Heating rate: 1 deg/min

Table 3 Comparison of the melting curves

	Ketoconazol	Cimetidin	
		0.11%*	0.97%*
W_T, K	0.74	1.02	1.92
T(Max)–T(0.5), K	0.0	0.1	0.3
R(Max)	0.64	0.71	0.85
s	-0.90	-1.90	-1.79

*impurity content

Such a sophisticated problem is paper ageing. On the one hand paper consists of a number of components, and the main component, cellulose is far from being chemically homogeneous, etc. On the other hand, ageing is an extremely complex process involving chemical reactions of cellulose and changes in the intramolecular and intermolecular interactions. Predicting the permanence (i.e. the resistance to ageing) or attempting to estimate the age of a paper requires methods to follow those complex changes.

An evolved gas analysis method was applied to follow the changes during the ageing of experimental and commercial papers [29]. Measurements were carried out on a Du Pont 916 Thermal Evolution Analyser detecting organic gases by means of a hydrogen flame ionization detector.

The EGA curves shown in Fig. 13 show that long time storage results in a shift of the peak towards lower temperatures and in a wider range of decomposition. These changes can be quantitatively described by parameters of peak position and width. Accelerated (thermal) ageing did not produce the same effect (see Table 4), though the deterioration of practical properties was greater after 120 hours at 100° than 25 years of natural ageing.

Table 4 Evaluation of EGA curves of an offset printing paper

	T(Max) °C	M_{1R} °C	ΔT(0.8, 0.2) °C	C_{2R} °C
original	320	314.4	25.9	284
natural ageing				
10 years	315	308.7	26.3	359
15 years	305	300.9	33.0	556
19 years	300	296.0	31.5	614
25 years	305	297.8	37.6	805
thermal ageing, 100°C, 50% r.h.				
4 h	320	314.7	27.4	452
8 h	320	312.8	26.5	414
24 h	320	314.5	26.8	428
72 h	320	312.8	26.6	417
120 h	320	313.8	26.0	390

Table 5 Evaluation of the EGA curves of a gravure printing paper containing mechanical pulp

	T(Max) °C	M_{1R} °C	ΔT(0.8, 0.2) °C	C_{2R} °C
original	315	312.3	28.8	529
natural ageing				
5 years	315	307.0	29.4	477
10 years	315	307.7	33.0	618
15 years	295	291.2	41.4	771
20 years	305	295.9	38.3	634
25 years	310	299.3	37.9	618

The data presented above are "lucky" to some extent, as for the homogeneous trend of changes. Owing to the complexity of the system, and, perhaps even more, to the changes in the source of cellulose and the technology (of the same paper quality) the trend is not always so clear. An example is shown in Table 5. Here, some sort of a turning point appeared near 15 years of age. (Of course, this does not mean that the microscopic transformations switched backwards.) However, the use of the empirical

parameters may, even is this case, help to characterize the overall process and to distinguish naturally and thermally aged paper samples.

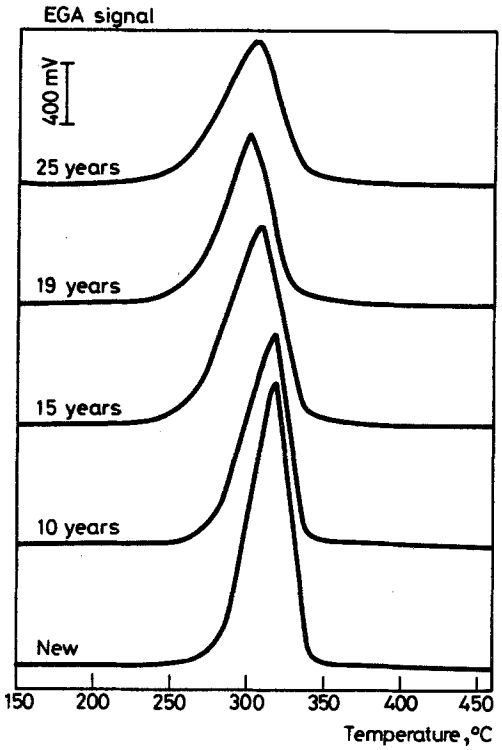

Fig. 13 EGA curves of an offset printing paper after natural ageing

Conclusion

The shape of peaks (or steps) of non-isothermal thermoanalytical curves can be described by empirical parameters, which are easy to calculate and do not require the assumption of a particular physical/chemical (e.g. kinetic) model. The empirical parameters can be applied to characterize the repeatability, reproducibility of curves, to describe the influence of different factors and processes (noise, baseline, kinetic constants, heat transfer etc.). Kinetic constants can be estimated on the basis of parameters characterizing peak position, width, asymmetry and sharpness. The empirical parameters are also suitable for a preliminary checking of experimental data prior to

calculations based on special models and for detecting minor changes and trends among samples of similar composition and structure.

A possible direction of further studies may be a search for more parameters which can contribute to the characterization of complex peaks with several maxima.

* * *

The authors express their thanks to Mrs E. Tóth for her valuable technical help.

The permission to reproduce Figs 2-6 and 8-10 from Analytica Chimica Acta and Thermochimica Acta (Elsevier, Amsterdam) is also acknowledged.

References

1 H. E. Kissinger, Anal. Chem., 29 (1957) 1702.
2 E. Koch, Non-Isothermal Reaction Analysis, Academic Press, London 1977.
3 E. Koch, Thermochim. Acta, 56 (1982) 1.
4 G. Várhegyi and T. Székely, Thermochim. Acta, 57 (1982) 13.
5 G. Pokol and S. Gál, Anal. Chim. Acta, 167 (1985) 183.
6 G. Pokol, S. Gál and E. Pungor, Anal. Chim. Acta, 167 (1985) 193.
7 G. Pokol, S. Gál and E. Pungor, Anal. Chim. Acta, 175 (1985) 289.
8 G. Pokol, S, Gál and E. Pungor, Thermochim Acta, 105 (1986) 313.
9 H. H. Horowitz and G. Metzger, Anal. Chem., 35 (1963) 1464.
10 M. Balarin, Thermochim. Acta, 33 (1979) 341.
11 G. E. Veress, A. Bezegh, L. Domokos, B. Kenderesy and P. Somogyvári, Research Report for ALUTERV-FKI, Technical Univ. of Budapest, Budapest, 1979.
12 H. G. McAdie, P. D. Garn and O. Menis, Selection of DTA temperature standards though a cooperative study (SRM 758, 759, 760), NBS Special Publ. 260-40 (1972).
13 B. Wunderlich and R. Bopp, J. Thermal Anal., 6 (1974) 335.
14 P. D. Garn and O. Menis, J. Macromol. Sci. - Phys., B13 (1977) 611.
15 G. Krien, Thermochim. Acta 20 (1977) 11.
16 R. L. Blaine, P. G. Fair, Thermochim. Acta 67 (1983) 233.
17 S. A. Moros, in Purity Determinations by Thermal Methods, ASTM STP 838, Ed: R. L. Blaine, C. K. Schoff, American Soc. for Testing and Materials, 1984, pp. 22-28.
18 S. Sarge and H. K. Cammenga, Thermochim. Acta, 94 (1985) 17.
19 G. W. H. Höhne, W. Eysel and K. H. Breuer, Thermochim. Acta, 94 (1985) 199.
20 B. C. Lippens, J. J. Steggerda, in Physical and Chemical Aspects of Absorbents and Catalysts, Ed.: B. G. Linsen, Academic Press, New York 1970, pp. 171-211.
21 A. V. Nikolaev and V. A. Logvinenko, J. Thermal Anal., 10 (1976) 363.
22 R. R. Krug, W. G. Hunter, R. A. Grieger, J. Phys. Chem., 80 (1976) 2335 and 2341.
23 M. Arnold, G. E. Veress, J. Paulik and F. Paulik, J. Thermal Anal., 17 (1979) 507.
24 N. Eisenreich, J. Thermal Anal., 19 (1980) 289.
25 J. Šesták, in Thermal Analysis, Proc. 6th Int. Conf., Vol. 1, Ed., H. G. Wiedemann, Birkhäuser Verlag, Basel 1980, p. 29.
26 M. Arnold,, G. E. Veress, J. Paulik and F. Paulik, Thermochim. Acta, 52 (1982) 67.
27 Z. Adonyi, Thermochim. Acta, 55 (1982) 269.
28 Z. Adonyi and G. Körösi, Thermochim. Acta, 60 (1983) 23.
29 F. Hevesi Tóth, G. Pokol, J. Györe and S. Gál, J. Thermal Anal., 33 (1988) 1153.

Zusammenfassung – Zur Beschreibung von Peaks bzw. Stufen thermoanalytischer Kurven wurden emperische Parameter ermittelt, die bei der Untersuchung der Reproduziertbarkeit, der Beziehung zwischen kinetischen Konstanten und Peakform so wie des Einflusses des thermischen Wiederstandes der Probe angewendet wurden. Kinetische Konstanten können auf der Basis von Peakformparametern geschätzt werden. Weiterhin wurden Kriterien für Experimente ermittelt, die eine kinetische Näherungslösung unter Vernachlässigung des Wärmetransportes innerhalb der Probe ermöglichen. Die empirischen Parameter wurden außerdem bei der Untersuchung der Eignung von DSC-daten zur Reinheitsanalyse angewendet, weiterhin zum Nachweis von alterungsbedingten Änderungen der thermischen Zerzetzung von Papier.